**Novel diagnosis- and progression-related microRNA signatures in melanoma**

Helena Gómez-Martínez[1,†], Borja Gómez-Cabañes[1,†], Adolfo López[1,2], Eva Hernando[3,*], Francisco García-García[1,*]

**Affiliations**

[1]Computational Biomedicine Laboratory, Principe Felipe Research Centre (CIPF), Valencia, Spain

[2]Joint unit in Biomedical Imaging FISABIO-CIPF, Foundation for the Promotion of Health and Biomedical Research of Valencia Region, Valencia, Spain

[3]Department of Pathology, New York University Grossman School of Medicine, New York, US

[†]These authors contributed equally to this work

**Corresponding authors:**

Eva Hernando, Eva.Hernando-Monge@nyulangone.org

Francisco García-García, fgarcia@cipf.es

**ORCiDs and email addresses:**

Helena Gómez-Martínez: https://orcid.org/0000-0001-8714-5197 (hegomezmartinez@gmail.com)

Borja Gómez-Cabañes: https://orcid.org/0000-0002-1126-5667 (bgomezc@cipf.es)

Adolfo López-Cerdán: https://orcid.org/0000-0001-9704-1877 (adlpecer@gmail.com)

Eva Hernando: https://orcid.org/0000-0003-1023-0312 (Eva.Hernando-Monge@nyulangone.org)

Francisco García-García: http://orcid.org/0000-0001-8354-5636 (fgarcia@cipf.es)

**Keywords**

Systematic review; meta-analysis; melanoma; transcriptomics; biomarkers; diagnosis; progression; microRNA

**ABSTRACT**

Melanoma, an aggressive skin cancer with a high mortality rate, has suffered from a recent increase in incidence; therefore, the search for biomarkers such as micro (mi)RNAs to aid the early detection and management of cancer patients represents a current concern.

To identify these potential biomarkers, we developed a novel and integrative strategy: we conducted a systematic review of melanoma studies following PRISMA guidelines and subsequently performed exploratory analysis and data normalization. Then, we performed individual analyses of each study followed by a miRNA meta-analysis that integrated all results while considering patient information.

In the diagnostic scenario, we unveiled twenty-four differentially expressed miRNAs - eleven upregulated and thirteen downregulated, with ten not previously directly related to the diagnosis of primary melanoma. In the ulceration scenario, we found twenty-three differentially expressed miRNAs - seven upregulated and sixteen downregulated, with thirteen not previously directly related to the diagnosis of primary melanoma. An extensive functional characterisation of these mirna signatures was carried out, providing insight into their biological role and impact on melanoma diagnosis and prognosis.

Our findings contribute to a better understanding of the molecular mechanisms and developmental processes involved in melanoma, mainly in early-stage development and ulceration, which, in turn, offers a means to develop novel resources for precisely detecting and treating melanoma.

## INTRODUCTION

Cutaneous melanoma, an aggressive skin cancer characterized by high metastatic potential and lethality, affects the pigment-producing cells on the skin surface and commonly presents symptoms that include alterations in the cells' size, shape, or color. Survival hinges on factors like Breslow's primary lesion thickness and early diagnosis, highlighting melanoma's aggressive nature. Indeed, melanoma accounts for about 5% of skin cancers yet contributes 80% of related deaths, particularly in fair-skinned populations (1,2,3,4).

Early-stage cutaneous melanoma, typically diagnosed during the radial growth phase, remains confined to the epidermis. Population-focused awareness campaigns targeting melanoma risks and clinical warning signs facilitate timely access to specialists for diagnosis and treatment; however, despite significant effort, the late onset of symptoms observed in a significant number of patients complicates early detection. In addition, molecular and clinical complexities contribute to immune evasion in melanoma, emphasizing the need for a comprehensive understanding of biological heterogeneity. Diagnosis relies on morphological analysis and visual examination supported by lesion dermoscopy and surgical intervention, which enhances early-stage survival rates; however, the metastatic potential associated with advanced disease considerably compromises these rates (5,6,7–11). Ulceration, characterized by skin breakdown over the melanoma lesion, correlates with poor clinical outcomes and represents the third most significant predictor of survival. Accurate staging and clinical management remain crucial, as ulceration significantly impacts disease prognosis (1, 2, 3).

MicroRNAs (miRNAs) - short non-coding RNAs that regulate the expression of genes associated with numerous biological processes - often suffer from disease-associated alterations in their expression profiles (16-19) and, as such, have vast potential as biomarkers for cancer diagnosis/prognosis. miRNA expression profiles frequently become dysregulated during cancer progression (including melanoma) (12,14,15), with distinct miRNA species already associated with cervical, breast, prostate, and esophageal cancers (A). In melanoma, previous studies have highlighted the downregulated expression of miRNAs such as miR-193a,

miR-338, and miR-565 in BRAF-mutant melanoma and the correlation of low miR-191 and high miR-193b expression with poor survival (20), and that miR-4286 affects melanoma cell proliferation and apoptosis by influencing multiple pathways (12). Studying alterations to miRNA expression profiles within melanoma tumor tissue may reveal novel molecular markers for disease diagnosis and progression (12); however, research gaps persist regarding the clinical utility of specific biomarkers compared with established outcome predictors (13) and the lack of effective biomarkers for early detection. We hypothesised that an integrative computational approach, which evaluates and combines all published datasets on miRNA expression in melanoma, may generate a consensus transcriptomic profile that improves our understanding of molecular mechanisms and regulatory processes, and lead to innovative strategies for early detection and treatment.

With this novel and integrative strategy we identify two relevant miRNA signatures: the first one focused on diagnosis included twenty-four differentially expressed miRNAs - eleven upregulated and thirteen downregulated, with ten not previously directly related to the diagnosis of primary melanoma. The second one related to the progression: we found twenty-three differentially expressed miRNAs - seven upregulated and sixteen downregulated, with thirteen not previously directly related to the diagnosis of primary melanoma. In addition, an extensive functional characterisation of these miRNA signatures was carried out, providing insight into their biological role and impact on melanoma diagnosis and prognosis.

## RESULTS

### Systematic review and meta-analysis of miRNA studies

Our systematic review initially identified fifty-seven studies from the Gene Expression Omnibus (GEO) and ArrayExpress (AE) databases. Based on the design criteria for eligibility, we included seven studies in this study (**Figure 1** describes the complete study selection).

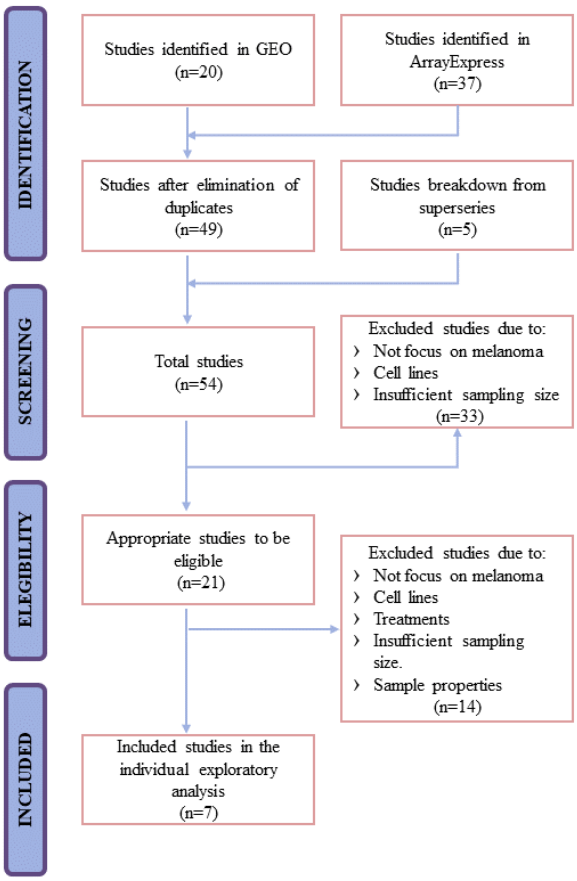


**Figure 1. Prisma diagram of the systematic review**

We considered two possible scenarios: a diagnostic scenario, comparing Primary cutaneous melanoma vs. Benign nevi (PM vs. BN), and an ulceration scenario, comparing Ulcerated melanoma vs. Non-ulcerated melanoma (UM vs. NUM). Finally, we also classified samples by patient resilience and included a survival context with the "Dead by melanoma vs. Alive" (DM vs. A) comparison. The studies involved in this research were published from 2010 to 2023, covering a total population of 397 subjects from seven studies, with miRNA expression detected in patients' skin tissue samples. We examined four studies for the ulceration scenario and three for the diagnosis scenario. Table S1 reports the main study characteristics, while Table S7 contains the differentially expressed miRNA analysis results. In the survival scenario, we compared 125 samples from DM patients with 129 samples from A patients (with or without the disease) from GSE59334,

GSE62370, and GSE62371; however, we found no significant results, although the meta-analysis strategy identified forty-seven differentially expressed miRNAs in melanoma patients.

**Figure S1** and **Table S8** report the meta-analysis results performed in diagnostic and ulceration scenarios. In the diagnostic scenario, we meta-analyzed 1127 miRNAs, unveiling twenty-four differentially expressed miRNAs - eleven upregulated and thirteen downregulated, with ten not previously directly related to the diagnosis of primary melanoma. In the ulceration scenario, we found twenty-three differentially expressed miRNAs - seven upregulated and sixteen downregulated, with thirteen not previously directly related to the diagnosis of primary melanoma.

**Table 1. Differentially-expressed miRNAs in the Primary melanoma vs. Benign nevus and Ulcerated vs. Non-ulcerated meta-analysis.** miRNAs in bold represent novel melanoma biomarkers for corresponding comparisons.

| Primary melanoma vs. Benign nevus | | | Ulcerated vs. Non-ulcerated | | |
|---|---|---|---|---|---|
| **miRNA** | **logFC** | **adjust p-value** | **miRNA** | **logFC** | **adjust p-value** |
| hsa-miR-1973 | 3.556 | 0.0002 | **hsa-miR-223-3p** | 1.494 | 0.007 |
| **hsa-miR-3648** | 3.34 | 0.0002 | **hsa-miR-196b-5p** | 1.351 | 0.037 |
| **hsa-miR-3156-5p** | 3.072 | 0.0120 | **hsa-miR-135b-5p** | 1.262 | 0.024 |
| **hsa-miR-3911** | 1.926 | 0.0040 | hsa-miR-363-3p | 1.195 | 0.021 |
| hsa-miR-21 | 1.776 | 0.0002 | hsa-miR-451 | 1.049 | 0.0001 |
| **hsa-miR-3610** | 1.275 | 0.0380 | hsa-miR-21 | 0.788 | 0.001 |
| hsa-miR-3138 | 1.274 | 0.0380 | hsa-miR-29a | 0.526 | 0.039 |
| hsa-miR-3195 | 1.156 | 0.0150 | hsa-miR-200c | -0.501 | 0.002 |
| hsa-miR-3132 | 0.999 | 0.0380 | **hsa-miR-5010-5p** | -0.511 | 0.048 |
| hsa-miR-142-5p | 0.814 | 0.0020 | **hsa-miR-301a-5p** | -0.515 | 0.024 |
| hsa-miR-22 | 0.754 | 0.0380 | **hsa-miR-450a-2-3p** | -0.539 | 0.039 |
| hsa-miR-23a | -0.561 | 0.0380 | **hsa-miR-580-3p** | -0.542 | 0.048 |
| **hsa-miR-30c** | -0.579 | 0.0190 | **hsa-miR-381-5p** | -0.545 | 0.04 |
| hsa-let-7d | -0.632 | 0.0020 | hsa-miR-203 | -0.561 | 0.019 |
| hsa-let-7c | -0.646 | 0.0380 | **hsa-miR-487b-5p** | -0.59 | 0.048 |
| hsa-miR-193b | -0.747 | 0.0002 | hsa-miR-205 | -0.593 | 0.019 |
| hsa-miR-508-3p | -1.04 | 0.0002 | **hsa-miR-552-3p** | -0.597 | 0.039 |
| hsa-miR-509-3p | -1.305 | 0.0002 | **hsa-miR-499a-5p** | -0.633 | 0.003 |
| hsa-miR-23b | -1.323 | 0.0002 | **hsa-miR-518e-3p** | -0.649 | 0.048 |
| hsa-miR-203 | -1.368 | 0.0160 | hsa-miR-489-3p | -0.659 | 0.048 |
| hsa-miR-205 | -1.571 | 0.0020 | **hsa-miR-133a-5p** | -0.667 | 0.019 |
| hsa-miR-100 | -1.7 | 0.0002 | hsa-miR-624-3p | -0.669 | 0.048 |
| hsa-miR-101 | -1.785 | 0.0002 | hsa-miR-376c-5p | -0.749 | 0.026 |
| hsa-miR-211 | -1.956 | 0.0080 | | | |

**Functional characterization of miRNA targets genes**

In the diagnostic scenario, we identified 15,684 target genes associated with differentially expressed miRNAs, while the number rose to 20,979 target genes in the ulcerated scenario. To understand the functional impact of these miRNAs and their target genes, we carried out extensive functional characterisation based on GO biological processes and Reactome pathways.

***Altered biological processes for the target genes in primary melanoma patients***

Based on the complete miRNA transcriptomic profile, we performed a GSEA on the biological process (BP) ontology of GO terms. In the diagnostic scenario, our functional analysis uncovers important altered biological functions involving the target genes, primarily highlighting perturbations in genetic information processing (**Figure 2A**). We identified disruptions in DNA repair and biosynthesis mechanisms, alongside chromatin modifications and increased mirRNA production, which impair DNA accessibility and promote gene silencing.. Furthermore, we observed a notable increase in mRNA catabolic processes alongside disturbances in mRNA stabilization within the poly(A) tail and the 3'- untranslated regions. We also identified functional disturbances associated with protein folding within the endoplasmic reticulum (ER) and disruptions to the cell cycle, specifically highlighting transcriptional impairments and anomalies in the G1 phase, along with altered apoptosis mechanisms and insulin receptors.

In order to obtain a more comprehensive and robust overview of the results we clusterised the full set of enriched biological functions, identifying significant alterations in several important functional groups (**Figure 2B**). The most prominent group corresponds to the genetic information processing as a central area of alteration (Cluster 1). Other notable clusters include signaling pathways and apoptosis (Cluster 2), cell cycle alterations (Cluster 4), cell growth and mobility dynamics (Cluster 3), and structural and organizational changes (Cluster 5).

To understand the relation and importance of the enriched biological functions we next constructed a similarity graph (**Figure 2C**). Most functional groups exhibit numerous internal connections, indicating potential functional interdependence. Notably, we observed a high number of connections between Cell cycle processes and Apoptosis, as well as between Protein phosphorylation and miRNA/mRNA processing. In contrast, clusters such as Signaling pathways and Development show fewer functional connections, suggesting that they are more independent, heterogeneous and isolated functional blocks.

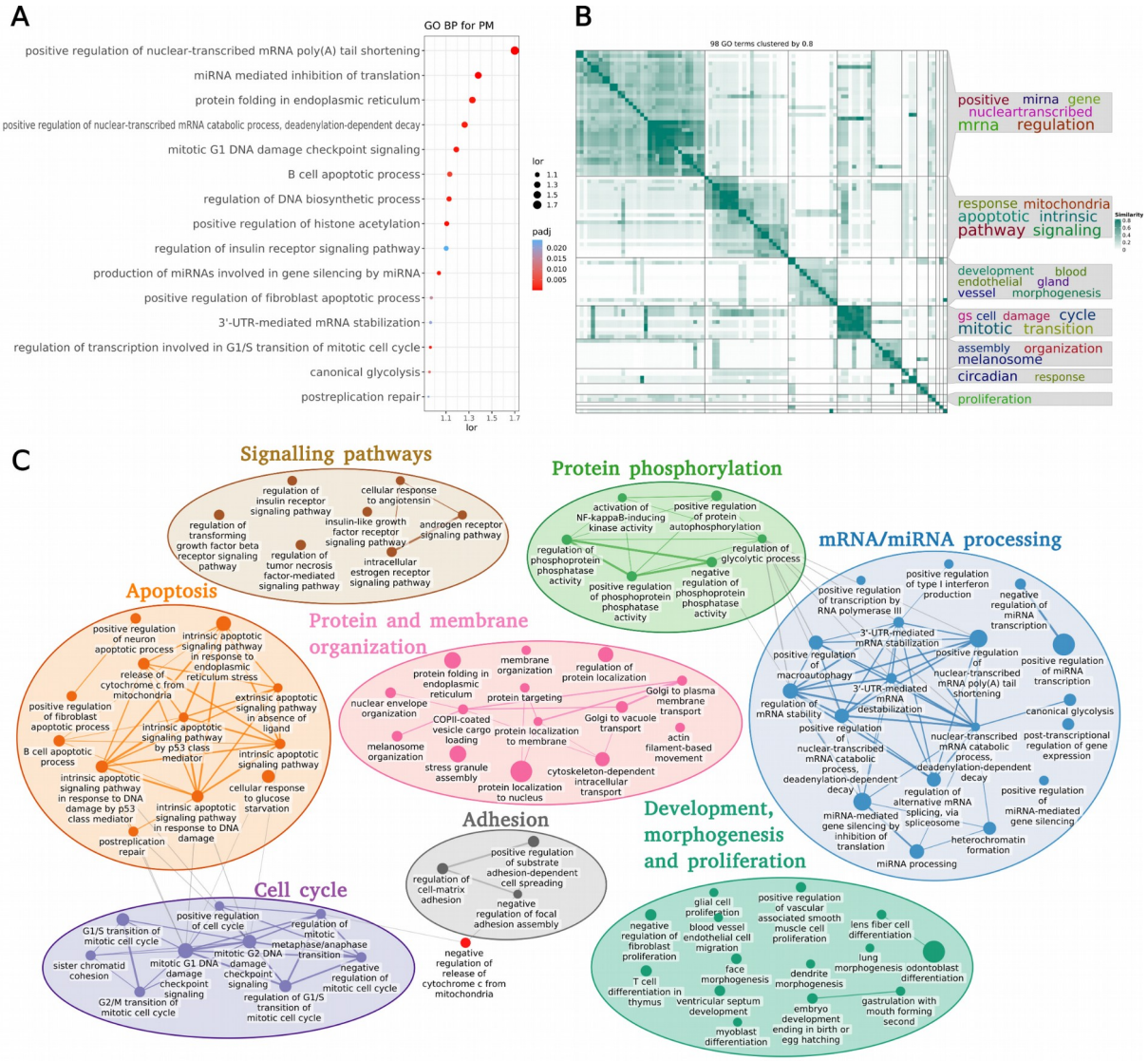


**Figure 2**. **Functional characterization with GO for the diagnostic scenario**. **A.** Dotplot displaying the fifteen most altered biological processes. **B.** Functional clustering for all significant biological processes (n = 98). Significantly

frequent words shown in the word cloud. **C.** Significant obtained terms. Each node is a GO term, while each axis is a relation between two terms. Thickness correlates with relationships. Node colors and groups represent a common functional theme.

***Altered biological processes for the target genes in the ulceration scenario***

In the ulceration scenario, we found that the most significantly altered biological functions (**Figure S2A**) involving target genes were similar to those identified in the diagnostic scenario - miRNA processing and silencing, altered mRNA stabilization and catabolism, and processes related to the cellular stress response such as ER overload.

The clustering of enriched biological functions in the ulceration scenario revealed a consistent pattern of significantly altered functional clusters, paralleling those identified in the diagnostic scenario (**Figure S2B**). Common clusters focus on critical aspects of cellular behavior, including post-transcriptional regulation (Cluster 1), cellular stress (Cluster 2), cell growth (Cluster 3), and cellular organization (Cluster 5). We observed a notable distinction in ulcerative melanoma in Cluster 1, with a marked tendency towards functions related to telomere regulation. Additionally, a more significant functional alteration in processes related to stress and cell damage (Clusters 2 and 6) underscored a heightened response to cellular damage in ulcerative melanoma, which may contribute to the aggressive behavior of the disease. Finally, the emergence of processes related to vesicular transport (Cluster 4) underscored the significance of cellular transport mechanisms in ulcerative melanoma.

We also constructed a graph of the enriched functions for the ulceration scenario (**Figure S2C**), unveiling a complex network of functional clusters categorizable into two principal groups. The first group (central to genetic information flow) featured a critical cluster focused on mRNA stabilization that links to lesser clusters, which reflects functional interdependence. The peripheral clusters support the existence of variations in telomeres and chromatin integrity alongside an upregulation in transcription and translation, which involve adjustments in post-transcriptional and post-translational mechanisms. The second major functional group complements the genetic information flow network with more generalized clusters, which

include those focused on cell growth and mobility dynamics. A trio of interconnected clusters dedicated to stress response, apoptosis, and cell cycle regulation emerge as a critical nexus, highlighting the integrated nature of cellular stress responses and their consequential impact on the cell cycle. A cluster focused on vesicular and protein transport displays close links to apoptosis; meanwhile, a smaller cluster related to cell adhesion and extracellular matrix interactions suggests the significance of cellular interactions with the microenvironment. The two main functional groups link through the cell cycle cluster and the protein phosphorylation and ubiquitination cluster, associating genetic information processing with cellular functions and revealing the complex molecular pathways influencing melanoma progression.

***Main biological REACTOME pathways altered***

Significantly altered pathways can be grouped into more general representative pathways (**Figure 3A**). These results highlighted genetic and metabolic alterations in both the diagnostic and ulceration scenarios. Our findings indicated generalized alterations in "Cell cycle," "Disease," "Transcription," "Immune System," "Programmed cell death," "Metabolism," and "Signal Transduction," with a higher intensity in the ulcerated scenario, accompanied by a remarkable stress response in pathways belonging to the functional groups "Cellular responses to stimuli" and alterations in "mitosis" and an alteration in "RNA polymerase II Transcription" (**Figure 3B**). In addition, we observed a reduction in cytosolic $Ca2^{+}$ levels in both scenarios and detected an increase in sensitivity to LDL in the specific case of ulceration.

The analyses also reveal general and protein-specific patterns of altered metabolism. Post-transcriptional modifications dominate the landscape in the diagnostic scenario, while lipid and carbohydrate metabolism alterations participate in the ulceration scenario (**Figure 3B**). "Cell signaling" and "vesicle-mediated transport" represent significantly altered functional clusters, particularly in the ulceration scenario. Finally, the ulceration scenario presents a series of unique functional groups, such as "Autophagy" and "Cell communication," – describing alterations in cell-extracellular matrix communication and hemidesmosome formation - "Organization of the extracellular matrix" - highlighting alterations with laminins, non-integrins,

and sidecans - and "Organelle biogenesis and maintenance" – relating to transcriptional changes associated with mitochondrial and cilia conformation.

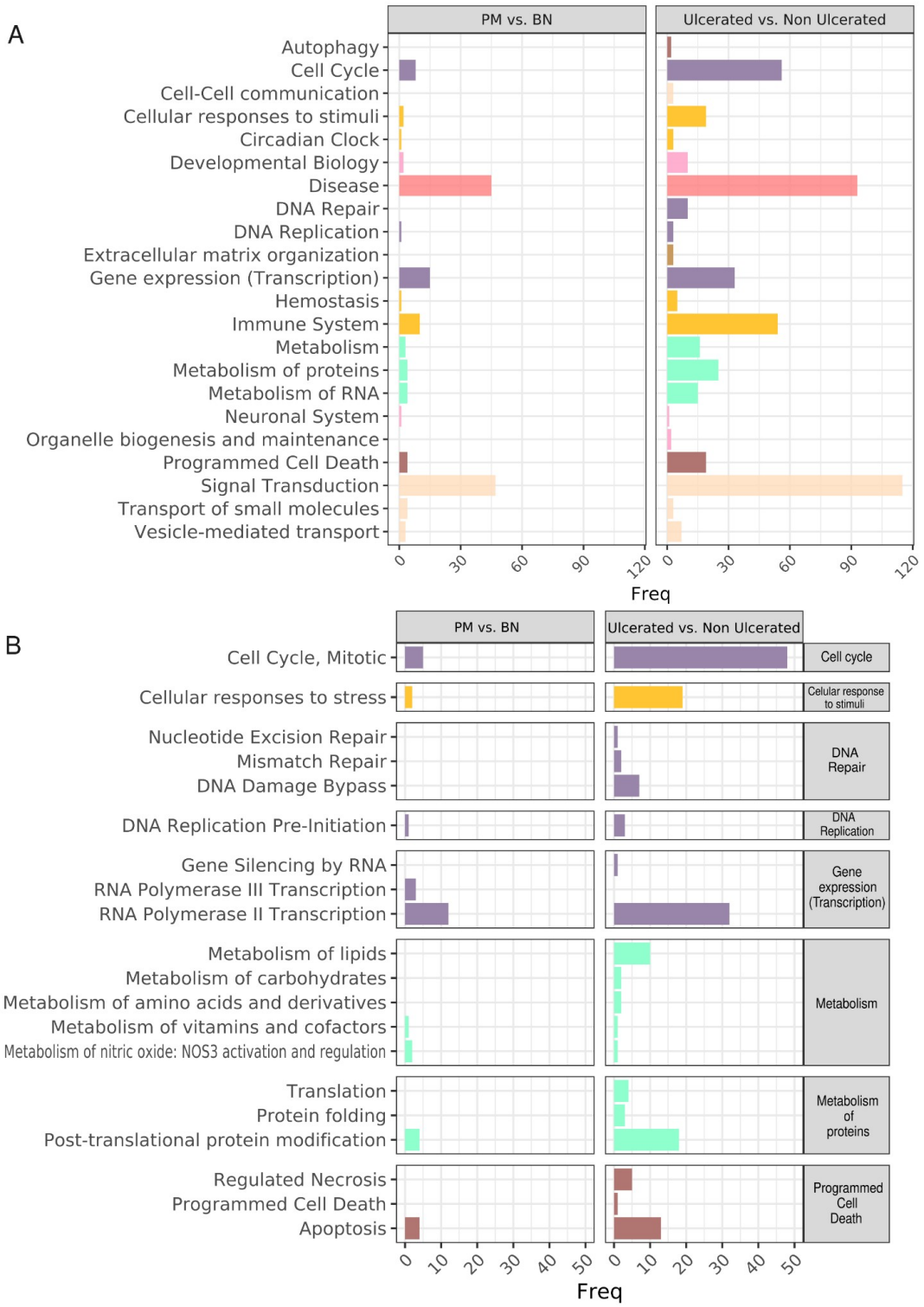

**Figure 3**. **Main biological REACTOME pathways altered. A.** Comprehensive overview of the abundance of significant pathways categorized based on their general group membership. **B.** Selected pathways of interest. On the right Y-axis, the primary group affiliations are depicted.

## Protein-Protein Interactions in Validated Target Genes for Melanoma

### *Cell cycle and stress response in primary melanoma*

In the diagnostic scenario, protein-protein interaction (PPI) network analysis for filtered target genes of upregulated miRNAs revealed a highly interconnected structure consisting of thirty-one genes (p-value: 2.46e-10) that formed a single central cluster, suggesting complex interactions among critical genes (**Figure 4A**). We identified four main functional modules within the network (**Table S2**): "Regulation and Cellular Development" (CASZ1, CCND1, BZW1, MAT2A, CDK6, POU2F1); Stress Response and Apoptosis (PTEN, CASP2, HIF1AN, PTBP1, MCL1, or AFF4), Cell Adhesion, Cell Junctions, and Extracellular Matrix (PTEN or PVR), and Immune system Regulation. These modules represent a functional signature highlighting several critical genes in the network, such as PTEN, HIF1A, CCND1, and CDK6. Functional dynamics suggest two main processes: epithelial tissue growth and expansion (indicated by the green group) and resistance and adaptation to stress conditions and apoptosis (represented by the red group). Next, we constructed a miRNA-miRNA target gene network comprising forty genes that successfully passed the same stringent filters (**Figure 4B**). This network prominently features hsa-miR-142-5p as the principal regulator (affecting a large number of genes) while hsa-miR-3156-5p, hsa-miR-3132, hsa-miR-3138, hsa-miR-3911, hsa-miR-3648, and hsa-miR-3195 play more secondary roles in terms of the number of regulated genes.

For the case of underexpressed miRNAs in the diagnostic scenario, six genes (NTRK3, CFTR, NFKB1, YAP1, C22orf2, FASLG) fulfilled all quality filters, which linked to hsa-miR-509-3p, hsa-miR-508-3p, hsa-miR-23b, hsa-miR-23a, hsa-let-7c, hsa-let-7d, hsa-miR-30c, and hsa-miR-101 (**Figure S2**).

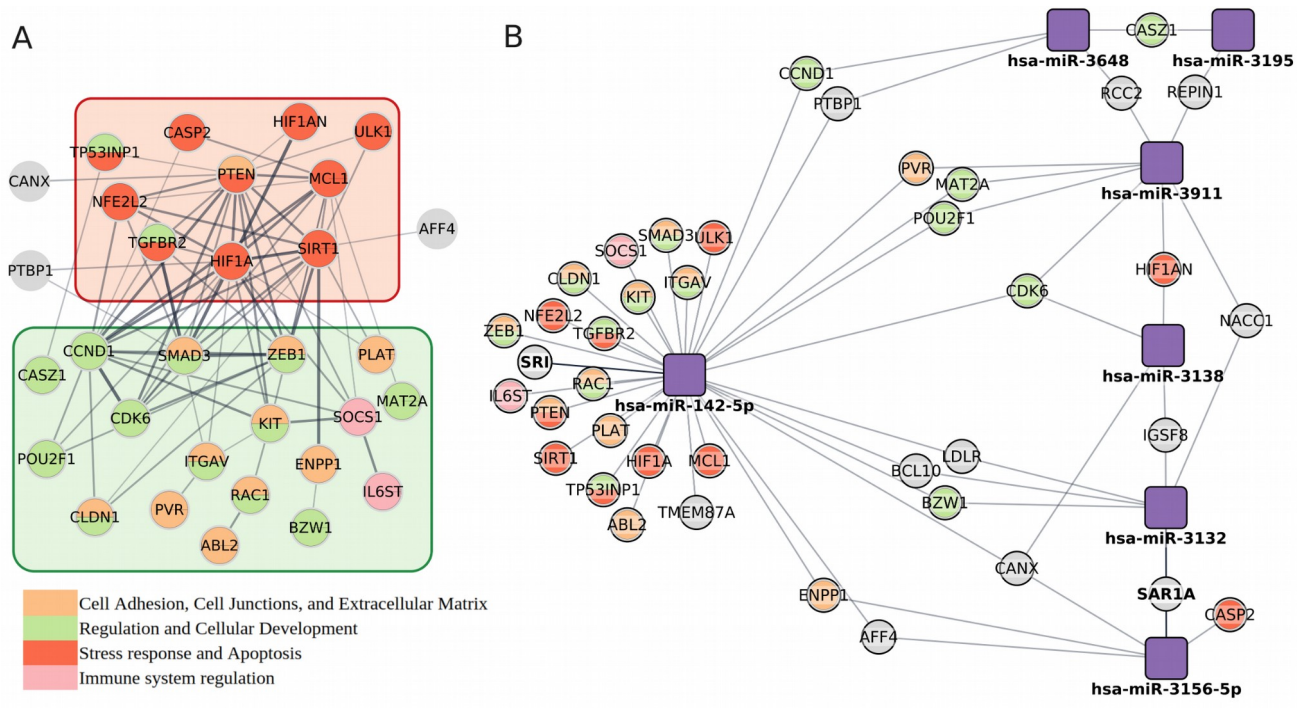


**Figure 4. Genes regulated by overexpressed miRNAs in the diagnostic scenario**. **A** Protein-protein interaction (PPI) network of filtered target genes relevant to the diagnosis scenario. Nodes represent a protein, and line (edge) indicates a biological interaction between proteins. Edge darkness correlates with interaction strength. Nodes are color-coded to represent different functional modules. The two large rectangles highlight the primary functional dynamics identified within the network - "epithelial tissue growth and expansion" in green and "resistance and adaptation to stress conditions and apoptosis" in red. **B** Significantly upregulated miRNAs in the diagnostic scenario along with corresponding target genes. Node colors denote the functional module to which each gene belongs. Genes in bold represent targets not previously associated with melanoma, as determined through comprehensive database filtering.

### *Immune activation and cell cycle in ulcerated melanoma*

In the ulceration scenario, the PPI network (p-value: 1.0E-16) constructed for the target genes of the upregulated miRNAs (**Figure 5A**) revealed eighty-five genes classified based on their functional processes and network topology into five significant clusters (**Table S3**): "Cell cycle" (CDK2, CDK4, CDK6, FBXW7, MDM2, or PTEN); "Immune response" (e.g., TWF1); "Genome regulation and maintenance" (CHUK, FOXO1,

FOXO3, SP1, or SP3); "Development and TGF-β/BMP" (ACVR1B, BGLAP, BMP2, BMPR2, ETS2, RUNX2, SKIL, SMAD5, SP7, TGFBR1), and "Development and Differentiation" (e.g., MAFB). The miRNA-miRNA target gene network we constructed (**Figure 5B**) underscored the pivotal role of miRNAs in ulceration. In this network, hsa-miR-223-3p represents a critical regulator, influencing genes within all five functional clusters but mainly targeting the immune system (yellow) and cell cycle (purple) clusters (analogous to the influence exerted by hsa-miR-36). Meanwhile, hsa-miR-135b-5p and hsa-miR-196b-5p specifically regulate genes linked to developmental processes. The constructed network also identified several genes (*SEPTIN2*, *CYB5A*, *SECISBP2L*, *CDS1*, *NUCKS1*, and *CNIH1*) previously unassociated with melanoma, suggesting new avenues for research while highlighting numerous well-established genes critical to cancer biology and development, emphasizing their regulation by the identified melanoma-associated miRNAs.

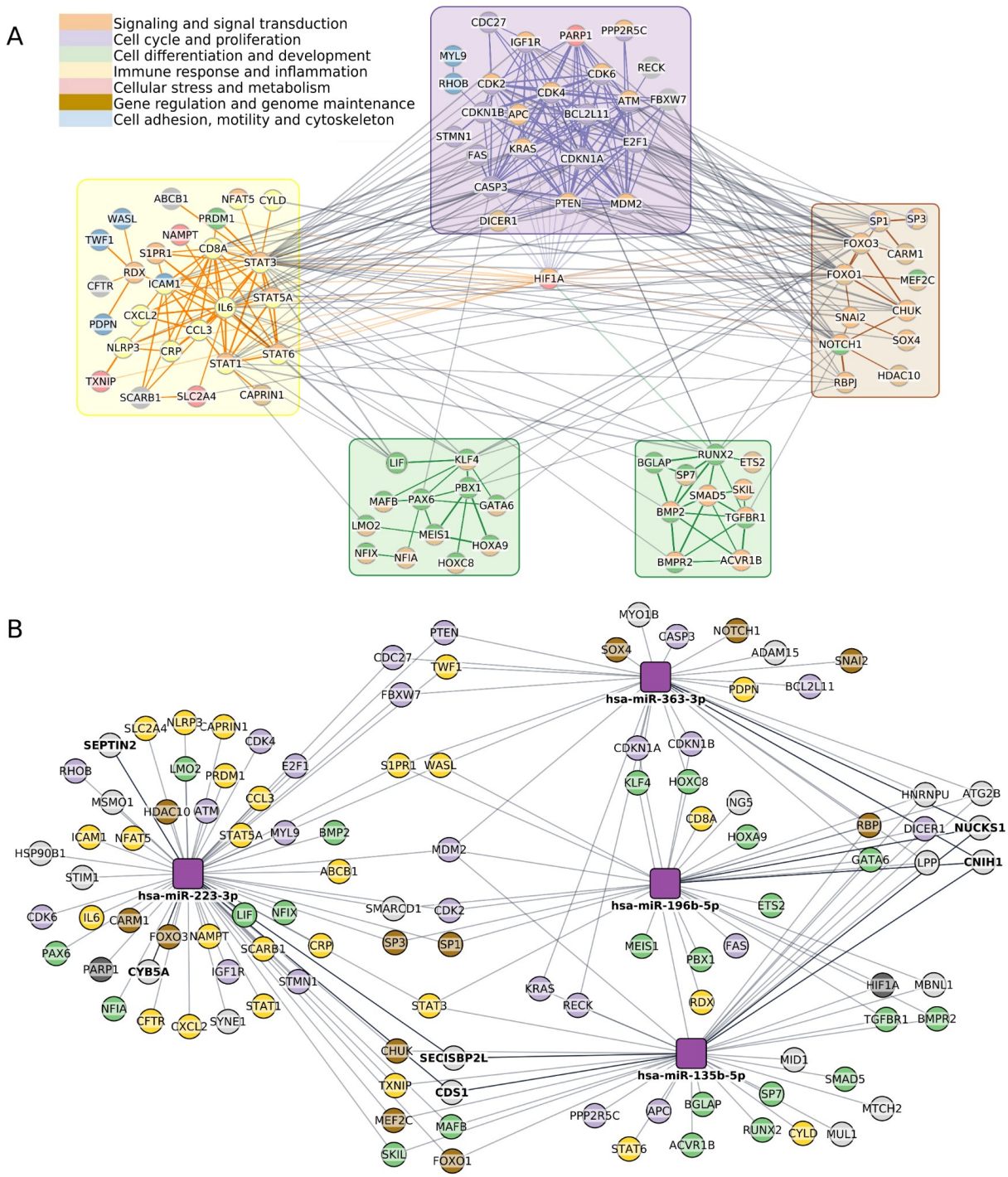


**Figure 5. Genes regulated by overexpressed miRNAs in the ulcerative scenario. A.** PPI network for genes regulated by overexpressed miRNAs in the ulcerative scenario. Node colors indicate general gene biological functions, with large squares forming clusters based on network topology: "Cell Cycle" (purple), "Immune System" (yellow), "Signal Transduction and Genome Maintenance" (brown), and "Cellular Differentiation and Proliferation" (green). Edge colors denote intragroup (rectangle color) or intergroup (gray) connections, revealing internal and cross-group node participation. Filters apply for nodes (minimum "Skin" expression of 2/5) and edges (minimum 0.6 confidence value).

**B.** Square nodes represent significantly overexpressed miRNAs in the ulcerative scenario, while circular nodes denote target genes. Edges depict miRNA-regulated gene relationships. For a circular node to be included, it requires a minimum 2/5 "Skin" expression. Circular node colors correspond to the assigned rectangular group in panel A. Some target genes (circular nodes) may not be present in panels A and B due to 1) links with other nodes being below 0.6 confidence, resulting in gene loss, 2) no connection with any gene, or 3) insufficient expression in Skin tissue. Circular node colors correspond to the assigned rectangular group in A. Bold nodes signify genes unrelated to melanoma in HMDD or MIRBASE.

For the case of underexpressed miRNAs in the ulceration scenario, we constructed the PPI network (p-value: 1.0E-16) (**Figure S3A**) with a total of thirty-eight genes, classified using the same functional pattern as for upregulated miRNAs. The genes in this network displayed a high level of connection, many playing central roles in critical biological processes; notable functions in this network include a critical dysregulation in genes such as *ERBB2*, *EGFR*, *IGF1R*, and *PIK3R2* that participate in the MAPK/ERK and PI3K/AKT pathways and cell communication and signal transduction, and, as such, are essential for tumor growth and progression. The interactions between significantly underexpressed miRNAs and their target genes in the ulceration scenario suggest uniform gene regulation (**Figure S3B**), in contrast to scenarios where a single upregulated miRNA is dominant in controlling multiple critical genes.

## DISCUSSION

Overall, the results obtained in our integrative strategy propose two novel miRNA signatures: hsa-miR-1973, hsa-miR-3648, hsa-miR-3156-5p, hsa-miR-3911, hsa-miR-3610, hsa-miR-3138, hsa-miR-3195, hsa-miR-3132 or hsa-miR-142-5p for the diagnosis of primary cutaneous melanoma and hsa-miR-223-3p, hsa-miR-196b-5p, hsa-miR-135b-5p, hsa-miR-363-3p, hsa-miR-451, and hsa-miR-29a for the identification of ulcerated primary cutaneous melanoma.

### *The role of novel miRNA biomarkers in melanoma diagnosis*

In the diagnostic scenario, we aimed to identify apparent differences attributed to the disease by comparing melanoma tissue with healthy tissue. We observed the significant alteration of twenty-four miRNAs (eleven upregulated, and thirteen downregulated), which agrees with previous research identifying miRNAs as diagnostic biomarkers for melanoma, including upregulated miRNAs such as hsa-miR-21 (14; 5, (2)), and downregulated miRNAs such as hsa-miR-211, hsa-miR-101, hsa-miR-100, hsa-miR-23b, hsa-miR-193b, hsa-let-7c, hsa-let-7d, hsa-miR-23a, hsa-miR-203, and hsa-miR-205 (reference; 3.; 1; 5.; 2; reference1; reference2). Additionally, our study in the diagnostic scenario also unveiled overexpressed miRNAs with no known association with melanoma diagnosis (e.g., hsa-miR-1973, hsa-miR-3648, hsa-miR-3156-5p, hsa-miR-3911, hsa-miR-3610, hsa-miR-3138, hsa-miR-3195, hsa-miR-3132, and hsa-miR-142-5p). Nevertheless, the significance and robustness of the meta-analysis, alongside validation through various techniques, suggest the importance of the activity of these microRNAs in melanoma, which affect the cell cycle and stress response functions.

The alteration of cell cycle pathways in primary melanoma tissue, particularly affecting processes in the G1/S phase, may involve hsa-miR-1973, which targets *CDK2AP1* and *RAB40C* to impact cell cycle dynamics and protein degradation mechanisms (reference1; Reference2;). hsa-miR-3648 and hsa-miR-142-5p target *CCND1*, with the encoded protein (Cyclin D1) playing a crucial role in cell cycle regulation through the modulation of cyclin-dependent kinases (CDKs) and having implications for poor prognosis in melanoma (Reference 1, Reference, 1; 1; 1). hsa-miR-3911 targets *CDK6*, indicating potential coordination with other miRNAs involved in cyclin regulation (e.g., hsa-miR-3138 and hsa-miR-142-5p). CDK6's significance in melanoma underscores its potential as a therapeutic target, with inhibitors showing promise in reducing tumor growth (Reference1; Reference2; Reference3; Reference4).

hsa-miR-3911 targets the critical cell cycle gene *RCC2*, crucial in cell division, suggesting a role in melanoma recurrence and poor prognosis (1 ;3), and *HIF1AN*, implying a possible downregulation and the subsequent elevation of HIF-1α activity, which can induce the epithelial-to-mesenchymal transition (EMT) in cancer cells and modulate the immune function of tumor cells, potentially facilitating immune evasion (( 2; 3; 5 ; (3).).

These findings collectively suggest a multifaceted role for miRNA hsa-miR-3911 in melanoma progression and therapy.

We found melanoma to be characterized not only by cell cycle alterations but also by disrupted apoptotic processes. hsa-miR-3648 and hsa-miR-142-5p target the *PTBP1* gene, known to regulate the expression of pyruvate kinase M2 isoform (PKM2) to influence cell proliferation, apoptosis, and metabolism (1;2;3;3). PTBP1's role in tumorigenesis involves apoptosis and cell cycle regulation, with caspase-3 and PARP1 becoming activated upon *PTBP1* downregulation, highlighting its intricate relationship with cancer progression (4; 5). Low *PTBP1* expression correlates with increased susceptibility to caspase-dependent apoptosis in cancer cells (4), promoting melanoma proliferation ((reference1; Reference2; Reference3; Reference4; Reference5; Reference6). Our findings suggest that caspases may play a role in melanoma development as programmed cell death pathways become altered, as evidenced by the upregulation of hsa-miR-3156-5p, which targets the *CASP2* gene, a known tumor suppressor in melanoma (3). While direct mutational inactivation of caspase-2 is unlikely, mechanisms such as miRNA-mediated or epigenetic silencing could explain its reduced expression (3). Our results indicate that hsa-miR-3156-5p may downregulate *CASP2* expression, potentially contributing to failed apoptosis and enhanced melanoma aggressiveness.

The *POU2F1* gene (targeted by hsa-miR-3911 and hsa-miR-142-5p) also alters apoptosis-related processes (Reference1) and affects DNA repair, which may prompt the high burden of somatic mutations in melanoma. The product of the *POU2F1* gene binds to the promoter region of Slc7a11 and regulates melanocytic cell development and progression (1; 2; 3; 5). hsa-miR-3911 and hsa-miR-142-5p also target PVR (the poliovirus receptor), which is overexpressed in many cancers and significantly impacts tumor cell behavior by promoting proliferation (1).

hsa-miR-3132 and hsa-miR-142-5p target *BCL10*, whose encoded protein participates in apoptosis and NF-kappaB (NF-κB) activation (Reference), suggesting a regulatory role in melanoma progression and highlighting possible immune system activation and cellular stress response in melanoma. These findings

support the connections between the cell cycle and apoptosis found through the functional enrichment analysis. hsa-miR-3911 and hsa-miR-3132 target *NACC1* (*Nucleus Accumbens-Associated Protein 1*) to increase NF-κB pathway signaling in melanoma cells, indicating a role in cancer progression (reference1; eference2; reference3; reference4; reference5). Regarding hsa-miR-3132, BCL10, and NACC1, this miRNA could have a significant role in NF-κB modulation. On the other hand, downregulation of hsa-miR-3156-5p is linked to JNK pathway activation and reduced JNK levels in various cancers (1). JNK interacts with AFF4, a target of hsa-miR-3156-5p and hsa-miR-142-5p, promoting melanoma cell progression (1). UV light exposure triggers JNK signaling pathway activation (1;2;3;4) and, combined with NF-κB, could support the immune responses and cellular stress associated with melanoma. The immune system represents a key altered pathway in primary melanoma and is influenced by hsa-miR-197 upregulation, which targets *IL17F*, an effector cytokine crucial for innate and adaptive immunity (PubMed:21350122).

Our study in the diagnostic scenario also highlighted functional disruptions related to protein folding within the ER in melanoma, as candidate melanoma biomarkers (hsa-miR-3138, hsa-miR-142-5p, and hsa-miR-3156-5p) target the *CANX* (or *CALX*) gene, which encodes an ER-associated protein involved in protein folding quality control (2 3 4 5 ). This suggests their potential as robust biomarkers for primary cutaneous melanoma diagnosis. Furthermore, *SAR1A* (targeted by hsa-miR-3156-5p and hsa-miR-3132) plays a critical role in ER homeostasis and COPII vesicle formation, indicating its significance in melanoma pathogenesis (Reference1; reference2; reference3; reference4).

Altered biological processes linked to metabolism and insulin receptors have been observed in primary melanoma. hsa-miR-3156-5p and hsa-miR-142-5p target *ENPP1* (Ectonucleotide Pyrophosphatase/Phosphodiesterase), a glycoprotein with pyrophosphatase and phosphodiesterase activity expressed in various cancer types (1 2 3 5 (3)). *ENPP1* expression in melanoma correlates with poor prognosis (1), while knockdown studies have indicated its potential to reduce metastasis, induce cell death, and enhance tumor responsiveness to immune checkpoint therapy (3). ENPP1's pivotal role in insulin signaling and action further underscores its significance in melanoma pathogenesis and therapy

(Reference1; Reference2; Reference3; Reference4). Continuing in this context of altered metabolism and insulin processing, hsa-miR-3138 and hsa-miR-3132 both target *IGSF8*, whose product regulates insulin-like growth factor-I (IGF-I) in melanoma cells, promoting their growth, survival, and migration and the production of the pro-inflammatory cytokine interleukin-8 (IL-8). Both insulin and IGFs represent essential regulators of energy metabolism and growth, and several findings have outlined their role in sporadic malignant melanoma (Reference1; Reference2; Reference3).

Our results also reflected an alteration of lipid metabolic pathways. hsa-miR-3132 and hsa-miR-142-5p target *LDLR* (Low-Density Lipoprotein Receptor), which encodes a protein involved in the uptake of LDL cholesterol from the bloodstream. *LDLR* expression becomes elevated in melanoma and has been related to LDL-mediated cancer growth in mice (4). hsa-miR-3132 and hsa-miR-142-5p algo target *BZW1* ((Basic Leucine Zipper and W2 Domains 1), which encodes a transcription factor that plays a significant role in various cancers, including melanoma (Reference1).

Our results also indicate that biological processes related to genetic information processing, DNA mechanisms, and genetic material biosynthesis become altered in melanoma. hsa-miR-3911 and hsa-miR-142-5p regulate the expression of the gene encoding MAT2A, an enzyme crucial for S-adenosylmethionine (SAM) synthesis, critical metabolite biosynthesis, gene expression regulation, and normal cellular function. *MAT2A* becomes downregulated in melanoma and non-small-cell lung cancer (2), which agrees with the findings of our study and suggests that hsa-miR-3911 upregulation may repress *MAT2A*, a synthetic lethal target in cancers with MTAP deletions, found in about 15% of all cancers (4; 5). hsa-miR-3195 and hsa-miR-3648 also have possible implications in genetic information processing as they share the target gene *CASZ1* (Castor Zinc Finger 1), which encodes a protein that plays crucial roles in various biological processes, including multicellular organism development, regulation of transcription, DNA-templating, and regulation of neuron differentiation (reference).

Of note, hsa-miR-3911, hsa-miR-142-5p, hsa-miR-3648, hsa-miR-3132, and hsa-miR-3195 all target one gene - *REPIN1*. This gene encodes the Replication Initiation Region Protein (60kD)( 2; 3), which is expressed in melanoma tissue samples (1).

While its role in melanoma remains unclear, hsa-miR-3911 holds promise as a candidate biomarker due to its involvement in various aspects and potential coordination with other miRNAs. Our findings also highlight hsa-miR-142-5p as a potentially exciting biomarker, given its expression in melanocytic tissue and targeting of multiple genes primarily expressed in skin tissue, characteristics shared by other melanoma-associated miRNAs (e.g., hsa-miR-3132, hsa-miR-3648, hsa-miR-3911, hsa-miR-3138, and hsa-miR-3156-5p).

***Understanding the miRNA signature in melanoma ulceration***

The presence of ulceration in melanoma correlates with unfavorable clinical outcomes and ranks as the third most potent predictor of survival in melanoma patients (reference). We compared ulcerated to non-ulcerated melanoma samples, revealing miRNAs such as has-miR-21, which displays upregulation in both cases and underscores the involvement of this miRNA in melanoma. Upregulated ulceration-associated miRNAs (e.g., hsa-miR-223-3p, hsa-miR-196b-5p, hsa-miR-135b-5p, hsa-miR-363-3p, hsa-miR-451, and hsa-miR-29a) have diverse roles in melanoma and share common target genes, indicating potential coordinated modulation in processes related to melanocytic skin ulceration (e.g., endoplasmic reticulum, apoptosis, cell cycle, cellular stress response, miRNA processing and silencing, or vesicular transport) that also become altered in the diagnostic scenario.

Protein metabolism functions relate to SUMOylation - a post-translational modification in which SUMO proteins become covalently attached to specific lysine residues in target proteins, thereby regulating various aspects of protein function (e.g., transcription, subcellular localization, DNA repair, and cell cycle (reference1; reference2)).

Studies have indicated that malignant melanoma exhibits heightened levels of autophagy, a cellular process involving the digestion of proteins/organelles to generate energy (Reference). Elevated autophagy levels correlate with diminished survival in metastatic melanoma patients, suggesting that autophagy could serve as a prognostic factor and a potential therapeutic target (Reference). Modified expression patterns of autophagy-associated genes (e.g., Beclin1 and LC3) have been observed in ulcerated melanoma, suggesting a plausible connection between autophagy and the aggressive histologic phenotype linked to ulceration (Reference).

As in our study, others have observed the upregulated expression of hsa-miR-223-3p in ulcerated compared to non-ulcerated melanoma (reference). hsa-miR-223-3p targets numerous genes involved in processes altered in ulcerated melanoma and shares target genes with miRNAs implicated in ulcerated melanoma. hsa-miR-196b-5p may have a multifaceted and context-dependent role in cancer biology, acting as an oncogene in melanoma but as a tumor suppressor in other cancer types, warranting further exploration of its mechanisms and potential as a biomarker or therapeutic target (reference; reference2, reference3). Evidence suggests that hsa-miR-135b-5p serves as a cancer type-/context-dependent oncogene or tumor suppressor. The upregulated expression noted in aggressive melanoma subtypes suggests further investigation to clarify the precise role of hsa-miR-135b-5p in melanoma (reference; reference2). hsa-miR-223-3p and hsa-miR-196b-5p both target *MDM2*, whose encoding protein participates in regulating the tumor suppressor protein p53 (overexpression enhances tumorigenisis) (Reference, Reference2).

hsa-miR-223-3p and hsa-miR-196b-5p affect gene silencing processes by targeting *SMARCD1* (also known as *BAF60A*), which belongs to the SWI/SNF family of chromatin remodeling complexes and participates in transcriptional activation and repression by chromatin remodeling, which alters DNA-nucleosome interaction to regulate gene expression (Reference).

As in the diagnostic scenario, cell cycle processes also become affected in the ulceration scenario, particularly those regulated by cyclins. hsa-miR-223-3p and hsa-miR-196b-5p target *CDK2*, which encodes a protein essential for the regulation of the G1 to S phase transition alongside cyclin A and E, and the CDK

inhibitors p21Cip1 and p27Kip1(Reference). Those both miRNAs algo target SP1 and SP3, two transcription factors that regulate the cell cycle and cell differentiation, SP1 and SP3 are constituents of the Sp family of transcription factors. SP3, involved in cell growth, differentiation, and apoptosis, is a protein-coding gene acting as a transcriptional activator, regulating the expression of target genes (Reference). SP1, also a protein-coding gene, is involved in gene expression regulation, functioning as a transcriptional activator by binding to GC boxes and regulating target gene expression [Reference2]. Despite their similar structures and high homology in DNA-binding domains, SP1 and SP3 exhibit strikingly distinct functions; furthermore, they play crucial roles in the hematopoietic specification, with SP3 partially compensating for SP1 in cells with disrupted SP1 DNA binding (Reference1, Reference2, reference3, reference4).

hsa-miR-223-3p targets *CD27* as does hsa-miR-363-3pb-5p. CD27 remains crucial in regulating T cell immunity, B cell activation, and overall immune system function, with potential implications for cancer immunotherapy (reference). Loss or inactivation of FBXW7 results in the accumulation of oncoproteins such as Cyclin E1, c-Myc, MCL1, mTOR, c-Jun, Notch1, p53, or SNAIL (reference).

hsa-miR-223-3p and hsa-miR-196b-5p share *STAT3* as a target gene with hsa-miR-135b-5p. STAT3 (Signal Transducer and Activator of Transcription 3) - a transcription factor pivotal in cell growth, survival, differentiation, inflammation, immune response, and apoptosis - becomes activated by phosphorylation in response to cytokines and growth factors, leading to dimerization, nuclear translocation, DNA binding, and gene transcription. (reference1; reference2; reference3; reference4; Reference). hsa-miR-223-3p and hsa-miR-135b-5p regulate the gene encoding the RNA binding protein SECISBP2L (Reference). While not directly implicated in melanoma ulceration according to the literature, our results suggest the potential involvement of SECISBP2L, given the association of hsa-miR-223-3p and hsa-miR-135b-5p in ulceration and the fact that RNA binding activity becomes altered in melanoma. We found a comparable situation with *SKIL* and *MAFB*, representing common targets of hsa-miR-223-3p and hsa-miR-135b-5p. SKIL promotes β-catenin signaling and participates in melanoma development; meanwhile, MAFB's exact role in melanoma

remains unclear, though expression in melanoma cells and tumor-associated macrophages suggests involvement in relevant cellular processes (reference; reference2).

hsa-miR-223-3p and hsa-miR-135b-5p may influence genome regulation and maintenance by targeting CHUK, a gene crucial to NF-κB signaling, which itself participates in melanoma development (reference). *FOXO1*, targeted by hsa-miR-223-3p and hsa-miR-135b-5p, encodes a tumor suppressor that includes apoptosis in cancer cells; in the context of ulceration, *FOXO1* functions to coordinate keratinocyte responses during wound healing (reference1, reference2). hsa-miR-223-3p and hsa-miR-135b-5p also regulate the *TXNIP* gene, whose downregulation may contribute to melanoma progression by affecting genes related to cell adhesion and the extracellular matrix (Reference). These reports underscore the relevance of these two miRNAs and potentially coordinated gene regulation in melanoma ulceration.

Researchers have also identified and previously implicated downregulated miRNAs in melanoma. Of the miRNAs identified in this study, hsa-miR-499a-5p becomes downregulated in melanoma tissues compared to benign nevi and correlates with poor prognosis, advanced clinical tumor-node-metastasis stage, and lymph node metastasis in melanoma patients (Referencia1, referecia2). Additionally, the MEL38 signature includes hsa-miR-624-3p, contributing to drug/immune resistance in melanoma (reference, reference2)). Moreover, hsa-miR-489-3p inhibits melanoma cell proliferation and glycolytic potential by targeting specific genes involved (reference1; reference2).

In summary, a specific microRNA has not yet been shown as an adequate marker to diagnose and predict the prognosis of melanoma patients; however, our findings underscore the complex regulatory networks orchestrated by miRNAs in melanoma pathogenesis and highlight their potential as diagnostic and therapeutic targets. Notably, we propose an miRNA signature for diagnosis in primary cutaneous melanoma: hsa-miR-1973, hsa-miR-3648, hsa-miR-3156-5p, hsa-miR-3911, hsa-miR-3610, hsa-miR-3138, hsa-miR-3195, hsa-miR-3132 or hsa-miR-142-5p. In addition, we propose the following miRNA-signature for ulcerated primary cutaneous melanoma: hsa-miR-223-3p, hsa-miR-196b-5p, hsa-miR-135b-5p, hsa-miR-363-3p, hsa-miR-451, and hsa-miR-29a. Nevertheless, our observations require further experimental

validation, mainly focusing on miRNAs with more significant log fold changes, such as hsa-miR-3648 or hsa-miR-223-3p, to ascertain their clinical relevance and utility.

## MATERIALS & METHODS

### Systematic review

The systematic review involved an exhaustive search for studies with miRNA microarray data in the GEO and AE repositories [Ref y Ref]. The search filters included the following keywords: melanoma, microRNAs, microRNA, miRNA, *Homo sapiens*, and expression profiling by array. The results obtained followed the inclusion criteria: (i) dataset type: "non-coding RNA profiling by array" and (ii) organism: "*Homo sapiens*." In the studies obtained through the search, filtering was carried out based on the following criteria: i) Focused on melanoma, ii) studies analyzing miRNAs, iii) tissue samples from *Homo sapiens* (excluding cell lines), iv) minimum sample size (minimum n = 12), v) samples without treatment, and v) not cell lines. Results were analyzed and presented following the PRISMA (Preferred Reporting Items for Systematic Reviews and Meta-Analyses) Guidelines (Page et al., 2021).

### Bioinformatic strategy for melanoma biomarkers identification

The workflow for each of the selected studies (Figure S4) was as follows: i) systematic review; ii) data acquisition, preprocessing, and normalization; iii) exploratory analysis; iv) data normalization; v) contrast groups and scenarios setting up and miRNA differential expression analysis; vi) miRNA meta-analysis; vii) functional enrichment; and viii) biological and clinical interpretation. Studies were grouped for meta-analysis based on tissue similarity and scenario of contrast.

### Data acquisition and preprocessing

After obtaining the selected studies, data was downloaded and individually analyzed to identify sample groups for future comparisons, incorporating them into a defined scenario. During this analysis, only *Homo*

*sapiens*-specific miRNAs were retained, and control probes were removed. Descriptive statistical analysis was then performed to detect anomalous data and behaviors and assess the distribution of various interest groups. After the individual exploratory analysis, unnormalized data from studies were standardized, and a Log2 transformation was applied if normalization was necessary. Samples exhibiting anomalous behavior were excluded from further analysis. This approach ensured that all selected studies began with normalized data to avoid introducing new biases and more significant variability in subsequent analyses.

All data processing was performed using the R programming language (R Core Team, 2021) from the RStudio graphical interface. The packages used for data download, processing, and analysis included the following: limma (Ritchie et al., 2015); ggplot2 (Wickham, 2009); dplyr (Wickham, 2021a); Biobase (Huber et al., 2015); factoextra (Kassambara and Mundt, 2020); impute (Hastie and Tibshirani, 2021), and stringr (Wickham, 2021b).

**miRNA differential expression and meta-analysis**

miRNA differential expression analysis was conducted individually for each study using the *limma* R package. Comparisons were made between the different groups defined in each study, as described in the previous section. The control group consisted of benign nevi, non-ulcerated melanoma cases, and living patients in each corresponding scenario. Meta-analyses were implemented with the R package metafor (Viechtbauer, 2010) under the DerSimonian & Laird random-effects model (DerSimonian R, Laird N (1986) Meta-analysis in clinical trials. Control Clin Trials 7:177–188. https://doi.org/10.1016/0197-2456(86)90046-2), considering individual study heterogeneity. This model considers the variability of individual studies by increasing the weights of studies with less variability when computing meta-analysis results. Thus, the most robust miRNAs between studies are highlighted. P-values, corrected p-values, LFC, LFC standard error (SE), and LFC 95% confidence intervals (CI) were calculated for each evaluated miRNA. miRNAs with corrected p-values lower than 0.05 were considered significant.

Three meta-analyses were performed, one for each scenario. The diagnostic scenario compared primary melanoma versus benign nevi (four studies). The ulceration scenario compared ulcerated and non-ulcerated primary cutaneous melanoma (four studies), while the survival comparison compared melanoma tissues from patients who had succumbed to the disease with those who successfully survived (three studies).

**Functional characterization of miRNAs targets genes**

To gain a deeper insight into the biological functions of the different scenarios, targets of the total miRNAs included in each meta-analysis were identified using the TarBase v8.0 [Ref] and miRTarBase v9.0 [Ref], which exclusively provide experimentally validated miRNA targets. A ranked list of genes was generated using these annotated target genes, and p-values and log fold changes (logFC) were derived. A Gene Set Analysis (GSA) was then conducted on the Gene Ontology (GO) [Ref] and REACTOME [Ref] databases using the logistic regression model implemented in the mdgsa R package [Ref] v0.99.2. Functional annotations were retrieved via the biomaRt package [Ref] 2.50.3 for the GO database and the Reactome.db package [Ref] v1.77.0 for the REACTOME database. The results were adjusted using the Benjamini-Hochberg (BH) method [Ref], and significance was determined with an adjusted p-value $< 0.05$. For scenarios with moderate significant results, such as diagnosis, a logFC cutoff of $\geq |0.5|$ was applied to identify pertinent terms without excessive representation. In scenarios with many significant terms, such as the ulcerated scenario, a stricter cutoff of $\geq |0.75|$ was implemented. These adjustments were crucial for managing data complexity and focusing the analysis on the most biologically relevant and impactful terms. For the visualization of the results, the simplifyEnrichment package [Ref] v1.10.0 was used to cluster and simplify the GO functional results, while the visualization of the GO terms network was accomplished using the REVIGO web tool [Ref] and Cytoscape v.3.10.1.

### *miRNA-target gene interactions*

For a more specific analysis, only the significant miRNAs in each scenario were selected, and the corresponding target genes were identified. Three critical filtering criteria were applied to refine the validity of miRNA-target interactions: i) targets with 'strong evidence' of validation, which includes reporter assays, Western blot, and qPCR (as documented in miRTarBase) and targets that received at least three validations categorized under 'less strong evidence,' ii) target recurrence among significant miRNAs, highlighting those targets most frequently repeated across our analyses, iii), implementing a gene expression filter utilizing stringApp [Ref] to discard target genes not exhibiting a minimum expression level of 2 out of 5 in skin tissue. This additional criterion ensured relevance and specificity to the physiological context. This final selection of genes and Cytoscape helped construct a PPI network that integrated high-confidence, experimentally validated interactions with biological relevance tailored to each scenario. In conjunction with this approach, a miRNA-target gene relationship network was constructed using Cytoscape to visualize the regulatory dynamics and interactions for each comparison between significant miRNAs and their targets after applying the critical filtering criteria.

## CONFLICT OF INTEREST

All the authors declare no conflict of interest.

## ACKNOWLEDGEMENTS

The authors thank the Principe Felipe Research Center (CIPF) for providing access to the cluster, co-funded by European Regional Development Funds (FEDER) in the Valencian Community 2014-2020. The authors also thank Stuart P. Atkinson for reviewing the manuscript.

## Funding

This research was supported by and partially funded by the Institute of Health Carlos III (project IMPaCT-Data, exp. IMP/00019), co-funded by the European Union, European Regional Development Fund (FEDER,

"A way to make Europe"), and PID2021-124430OA-I00 funded by MCIN/AEI/10.13039/501100011033/ FEDER, UE ("A way to make Europe"). Borja Gómez-Cabañes is supported by a PhD fellowship funded by the Spanish Association Against Cancer in Valencia (PRDVA234163GOME).

**Data availability**

The data used for the analyses described in this work are publicly available at GEO and AE repositories [Ref and Ref]. The accession numbers of the GEO datasets downloaded are GSE18509, GSE34460, GSE59334, GSE62370, GSE62371, GSE211090, and GSE211092. The accession number of the AE datasets downloaded is EMTAB4915.

**REFERENCES**

1. Sandru A, Voinea S, Panaitescu E, Blidaru A. Survival rates of patients with metastatic malignant melanoma. J Med Life [Internet]. Carol Davila - University Press; 2014 [cited 2023 Jan 2]; 7:572. Available from: /pmc/articles/PMC4316142/
2. Atkins MB, Curiel-Lewandrowski C, Fisher DE, Swetter SM, Tsao H, Aguirre-Ghiso JA, et al. The State of Melanoma: Emergent Challenges and Opportunities. Clin Cancer Res [Internet]. Clin Cancer Res; 2021 [cited 2022 Jan 30];27:2678–97. Available from: https://pubmed.ncbi.nlm.nih.gov/33414132/
3. O'Shea SJ, Rogers Z, Warburton F, Ramirez AJ, Newton-Bishop JA, Forbes LJL. Which symptoms are linked to a delayed presentation among melanoma patients? A retrospective study. BMC Cancer [Internet]. BioMed Central Ltd.; 2017 [cited 2023 Jan 2];17:1–6. Available from: https://bmccancer.biomedcentral.com/articles/10.1186/s12885-016-2978-6
4. Naik PP, Naik PP. Cutaneous Malignant Melanoma: A Review of Early Diagnosis and Management. World J Oncol [Internet]. 2021 [cited 2023 Jan 2];12:7–19. Available from: https://www.wjon.org/index.php/wjon/article/view/1349
5. Goyal M, Knackstedt T, Yan S, Hassanpour S. Artificial intelligence-based image classification methods for diagnosis of skin cancer: Challenges and opportunities. Comput Biol Med [Internet]. Comput Biol Med; 2020 [cited 2023 Jan 2];127. Available from: https://pubmed.ncbi.nlm.nih.gov/33246265/
6. Kaiser S, Vassell R, Pinckney RG, Holmes TE, James TA. Clinical impact of biopsy method on the quality of surgical management in melanoma. J Surg Oncol [Internet]. J Surg Oncol; 2014 [cited 2023 Jan 2];109:775–9. Available from: https://pubmed.ncbi.nlm.nih.gov/24862925/
7. Fares J, Fares MY, Khachfe HH, Salhab HA, Fares Y. Molecular principles of metastasis: a hallmark of cancer revisited. Signal Transduction and Targeted Therapy 2020 5:1 [Internet]. Nature Publishing Group; 2020 [cited 2023 Jan 2];5:1–17. Available from: https://www.nature.com/articles/s41392-020-0134-x
8. Kirstein JM, Hague MN, McGowan PM, Tuck AB, Chambers AF. Primary melanoma tumor inhibits metastasis through alterations in systemic hemostasis. J Mol Med (Berl) [Internet]. J Mol Med (Berl); 2016 [cited 2023 Jan 2];94:899–910. Available from: https://pubmed.ncbi.nlm.nih.gov/27048169/
9. Nirschl CJ, Suárez-Fariñas M, Izar B, Prakadan S, Dannenfelser R, Tirosh I, et al. IFNγ-Dependent Tissue-Immune Homeostasis Is Co-opted in the Tumor Microenvironment. Cell [Internet]. Cell; 2017 [cited 2023 Jan 2];170:127-141.e15. Available from: https://pubmed.ncbi.nlm.nih.gov/28666115/

10. Neagu M, Constantin C, Tanase C. Immune-related biomarkers for diagnosis/prognosis and therapy monitoring of cutaneous melanoma. Expert Rev Mol Diagn [Internet]. Expert Rev Mol Diagn; 2010 [cited 2023 Jan 2];10:897–919. Available from: https://pubmed.ncbi.nlm.nih.gov/20964610/
11. Erdei E, Torres SM. A new understanding in the epidemiology of melanoma. Expert Rev Anticancer Ther [Internet]. NIH Public Access; 2010 [cited 2022 Jan 28];10:1811. Available from: /pmc/articles/PMC3074354/
12. Komina A, Palkina N, Aksenenko M, Tsyrenzhapova S, Ruksha T. Antiproliferative and Pro-Apoptotic Effects of MiR-4286 Inhibition in Melanoma Cells. PLoS One [Internet]. Public Library of Science; 2016 [cited 2023 Jan 2];11:e0168229. Available from: https://journals.plos.org/plosone/article?id=10.1371/journal.pone.0168229
13. Swetter SM, Tsao H, Bichakjian CK, Curiel-Lewandrowski C, Elder DE, Gershenwald JE, et al. Guidelines of care for the management of primary cutaneous melanoma. J Am Acad Dermatol [Internet]. J Am Acad Dermatol; 2019 [cited 2023 Jan 2];80:208–50. Available from: https://pubmed.ncbi.nlm.nih.gov/30392755/
14. Mueller DW, Rehli M, Bosserhoff AK. miRNA expression profiling in melanocytes and melanoma cell lines reveals miRNAs associated with formation and progression of malignant melanoma. J Invest Dermatol [Internet]. J Invest Dermatol; 2009 [cited 2023 Jan 2];129:1740–51. Available from: https://pubmed.ncbi.nlm.nih.gov/19212343/
15. Jayawardana K, Schramm SJ, Tembe V, Mueller S, Thompson JF, Scolyer RA, et al. Identification, Review, and Systematic Cross-Validation of microRNA Prognostic Signatures in Metastatic Melanoma. J Invest Dermatol [Internet]. J Invest Dermatol; 2016 [cited 2023 Jan 2];136:245–54. Available from: https://pubmed.ncbi.nlm.nih.gov/26763444/
16. Ambros V. microRNAs: tiny regulators with great potential. Cell [Internet]. Cell; 2001 [cited 2023 Jan 2];107:823–6. Available from: https://pubmed.ncbi.nlm.nih.gov/11779458/
17. Bartel DP. MicroRNAs: Genomics, Biogenesis, Mechanism, and Function. Cell [Internet]. Cell Press; 2004 [cited 2023 Jan 2];116:281–97. Available from: https://pubmed.ncbi.nlm.nih.gov/14744438/
18. He L, Hannon GJ. MicroRNAs: small RNAs with a big role in gene regulation. Nature Reviews Genetics 2004 5:7 [Internet]. Nature Publishing Group; 2004 [cited 2023 Jan 2];5:522–31. Available from: https://www.nature.com/articles/nrg1379
19. Gaur A, Jewell DA, Liang Y, Ridzon D, Moore JH, Chen C, et al. Characterization of microRNA expression levels and their biological correlates in human cancer cell lines. Cancer Res [Internet]. Cancer Res; 2007 [cited 2023 Jan 2];67:2456–68. Available from: https://pubmed.ncbi.nlm.nih.gov/17363563/
20. Caramuta S, Egyházi S, Rodolfo M, Witten D, Hansson J, Larsson C, et al. MicroRNA expression profiles associated with mutational status and survival in malignant melanoma. J Invest Dermatol [Internet]. J Invest Dermatol; 2010 [cited 2023 Jan 2];130:2062–70. Available from: https://pubmed.ncbi.nlm.nih.gov/20357817/
21. Frampton AE, Gall TM, Castellano L, Stebbing J, Jiao LR, Krell J. Towards a clinical use of miRNAs in pancreatic cancer biopsies. http://dx.doi.org/101586/erm12136 [Internet]. Taylor & Francis; 2014 [cited 2023 Jan 2];13:31–4. Available from: https://www.tandfonline.com/doi/abs/10.1586/erm.12.136
22. Drahos J, Schwameis K, Orzolek LD, Hao H, Birner P, Taylor PR, et al. MicroRNA Profiles of Barrett's Esophagus and Esophageal Adenocarcinoma: Differences in Glandular Non-native Epithelium. Cancer Epidemiol Biomarkers Prev [Internet]. Cancer Epidemiol Biomarkers Prev; 2016 [cited 2023 Jan 2];25:429–37. Available from: https://pubmed.ncbi.nlm.nih.gov/26604271/
23. Sand M, Skrygan M, Sand D, Georgas D, Gambichler T, Hahn SA, et al. Comparative microarray analysis of microRNA expression profiles in primary cutaneous malignant melanoma, cutaneous malignant melanoma metastases, and benign melanocytic nevi. Cell Tissue Res [Internet]. Cell Tissue Res; 2013 [cited 2023 Jan 2];351:85–98. Available from: https://pubmed.ncbi.nlm.nih.gov/23111773/
24. Burns D, George J, Aucoin D, Bower J, Burrell S, Gilbert R, et al. The Pathogenesis and Clinical Management of Cutaneous Melanoma: An Evidence-Based Review. J Med Imaging Radiat Sci

[Internet]. J Med Imaging Radiat Sci; 2019 [cited 2023 Jan 2];50:460-469.e1. Available from: https://pubmed.ncbi.nlm.nih.gov/31204313/